Figure S1

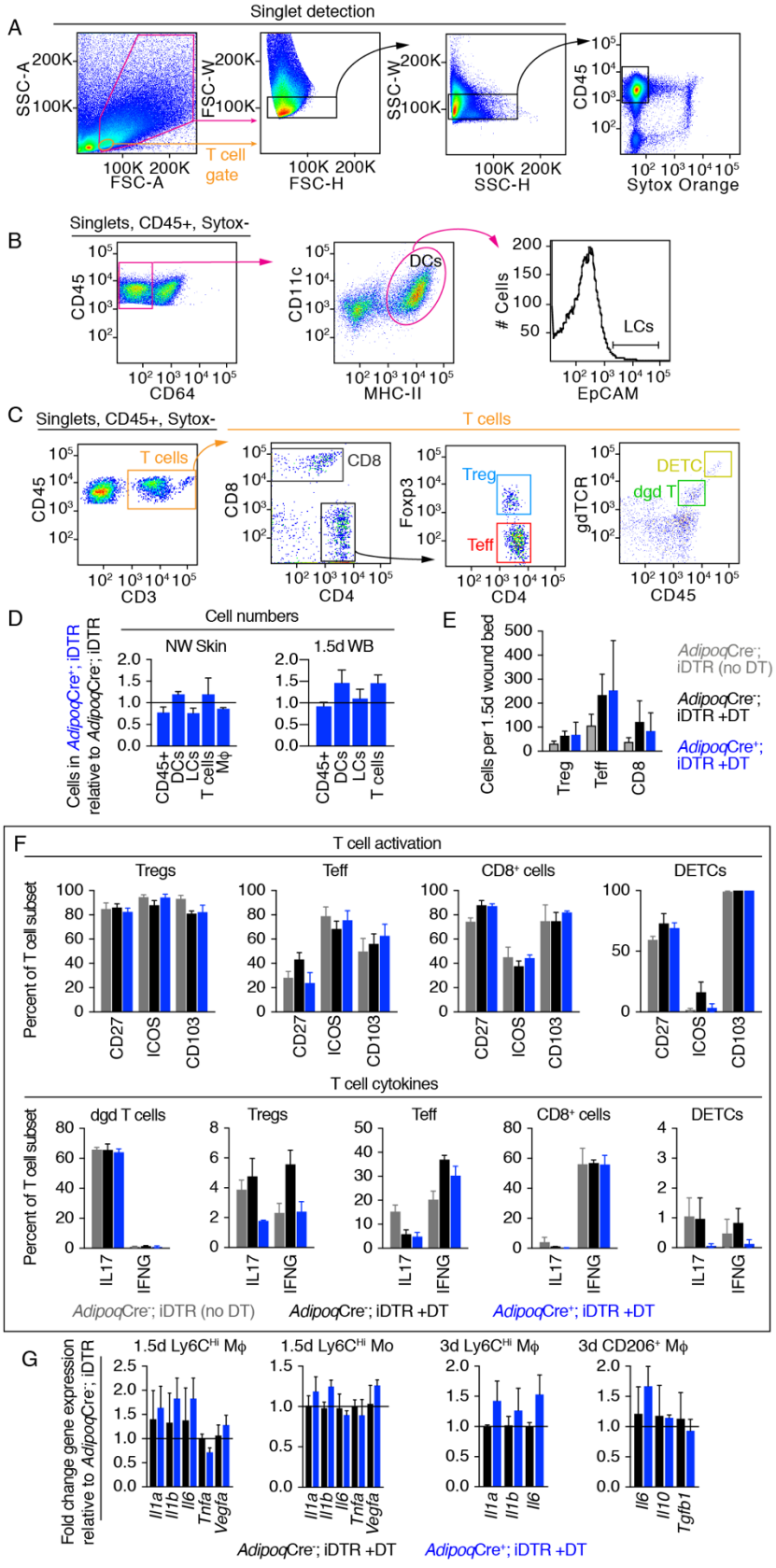
A
Singlet detection
SSC-A
FSC-A
T cell gate
FSC-W
FSC-H
SSC-W
SSC-H
CD45
Sytox Orange
B
Singlets, CD45+, Sytox-
CD64
MHC-II
DCs
Cells
EpCAM
LCs
C
Singlets, CD45+, Sytox-
T cells
CD3
CD4
CD8
Treg
Teff
Foxp3
gdTCR
DETC
dgd T
D
Cell numbers
NW Skin
1.5d WB
Cells in AdipoqCre+; iDTR relative to AdipoqCre-; iDTR
CD45+
DCs
LCs
T cells
Mφ
E
Cells per 1.5d wound bed
Treg
Teff
CD8
AdipoqCre-; iDTR (no DT)
AdipoqCre-; iDTR +DT
AdipoqCre+; iDTR +DT
F
T cell activation
Tregs
Teff
CD8+ cells
DETCs
Percent of T cell subset
CD27
ICOS
CD103
T cell cytokines
dgd T cells
IL17
IFNG
AdipoqCre-; iDTR (no DT)
AdipoqCre-; iDTR +DT
AdipoqCre+; iDTR +DT
G
1.5d Ly6CHi Mφ
1.5d Ly6CHi Mo
3d Ly6CHi Mφ
3d CD206+ Mφ
Fold change gene expression relative to AdipoqCre-; iDTR
Il1a
Il1b
Il6
Tnfa
Vegfa
Il10
Tgfb1
AdipoqCre-; iDTR +DT
AdipoqCre+; iDTR +DT

Figure S1. Immune cell characterization in wound beds from dermal adipocyte depleted mice. Related to Figure 1.

(A-C) Flow cytometry plots to detect non-dead CD45+ immune cell singlets (A), dendritic cells (DC) and Langerhans cells (LC) (B), and different T cell subsets (C). (D) Quantification of immune cell subsets in nonwounded (NW) skin and 1.5-day wound beds from *Adipoq*Cre+; iDTR mice relative to the same *Adipoq*Cre-; iDTR mice (*n* = 3-4 mice for each condition and time point). (E-F) Quantification of T cell subsets (E) and the percentage of each subset that is positive for different activation/phenotype markers (F) in 1.5-day wound beds (*n* = 3-5 mice for each condition). (G) Quantitative real-time PCR of inflammatory gene expression in macrophages and monocytes from day 1.5 and 3 wound beds of *Adipoq*Cre+; iDTR mice relative to time point matched wound beds of *Adipoq*Cre-; iDTR mice (*n* = 3 mice for each time point). Error bars indicate mean ± SEM. Mϕ, macrophage; Mo, monocyte; DETC, dendritic epidermal T cell; dgd T, dermal gamma-delta T cell; WB, wound bed; DT, diphtheria toxin.

Figure S2

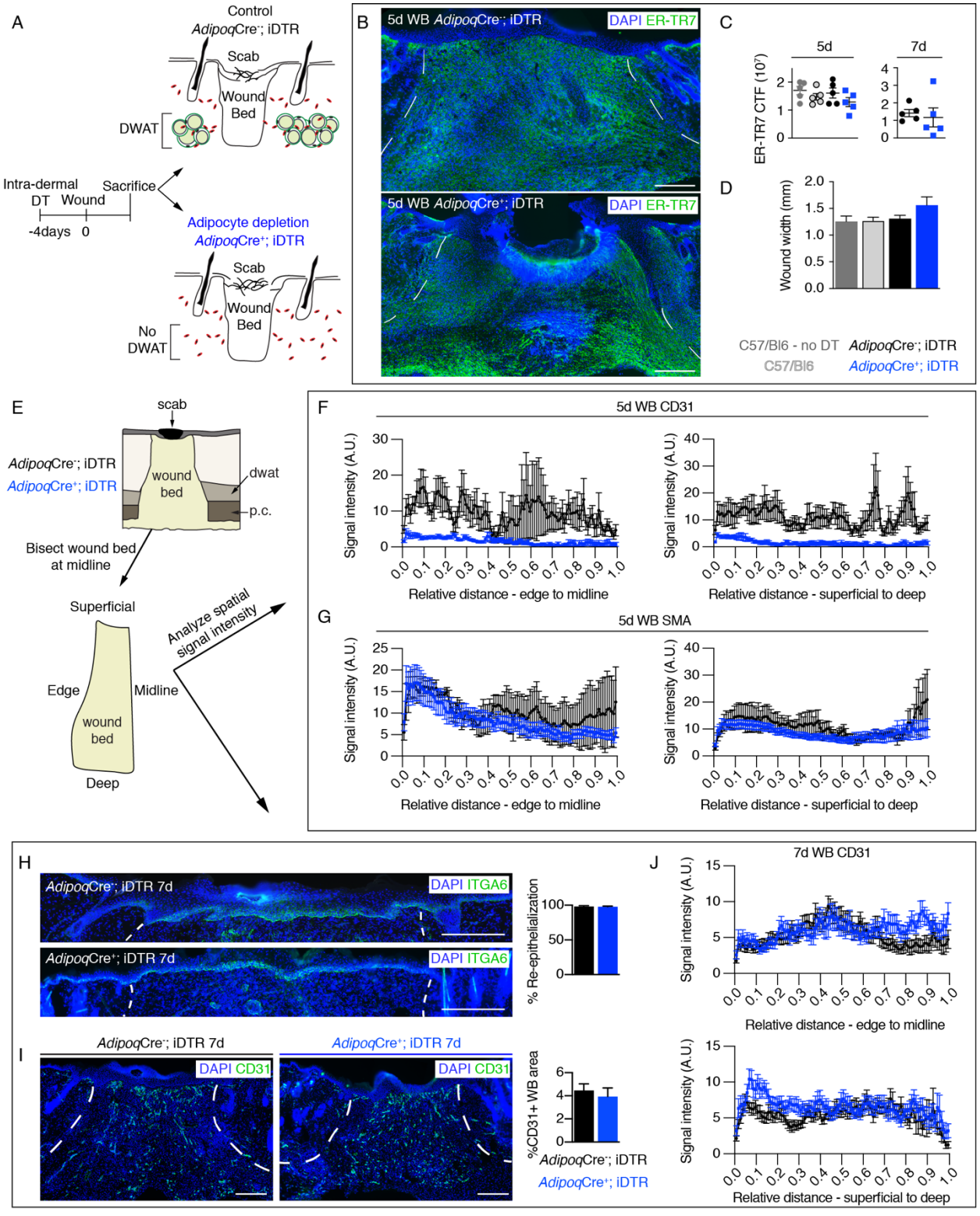
A
Control
AdipoqCre-; iDTR
Scab
Wound Bed
DWAT
Intra-dermal DT
Wound
Sacrifice
-4days
0
Adipocyte depletion
AdipoqCre+; iDTR
Scab
Wound Bed
No DWAT
B
5d WB AdipoqCre-; iDTR
DAPI ER-TR7
5d WB AdipoqCre+; iDTR
DAPI ER-TR7
C
5d
7d
ER-TR7 CTF (10^7)
D
Wound width (mm)
C57/Bl6 - no DT
AdipoqCre-; iDTR
C57/Bl6
AdipoqCre+; iDTR
E
scab
AdipoqCre-; iDTR
AdipoqCre+; iDTR
wound bed
dwat
p.c.
Bisect wound bed at midline
Superficial
Edge
Midline
wound bed
Deep
Analyze spatial signal intensity
F
5d WB CD31
Signal intensity (A.U.)
Relative distance - edge to midline
Relative distance - superficial to deep
G
5d WB SMA
Signal intensity (A.U.)
Relative distance - edge to midline
Relative distance - superficial to deep
H
AdipoqCre-; iDTR 7d
DAPI ITGA6
AdipoqCre+; iDTR 7d
DAPI ITGA6
% Re-epithelialization
I
AdipoqCre-; iDTR 7d
AdipoqCre+; iDTR 7d
DAPI CD31
DAPI CD31
%CD31+ WB area
AdipoqCre-; iDTR
AdipoqCre+; iDTR
J
7d WB CD31
Signal intensity (A.U.)
Relative distance - edge to midline
Relative distance - superficial to deep

Figure S2. Delayed revascularization and re-epithelialization are corrected in wound beds from dermal adipocyte depleted mice. Related to Figure 1.

(A) Strategy to ablate dermal adipocytes and schematic of skin following dermal adipocyte depletion. (B-D) Composite images from ER-TR7 immunostained sections (B) and quantification of corrected total fluorescence (fibroblast repopulation) in wound beds (C) and calculated wound width (D) ($n \geq 5$ mice for each condition). (E) Pipeline for processing immunostained tissue sections to quantify the spatial distribution of fluorescent signal. (F-G) Spatial distribution of CD31 (F) and SMA (G) signal in 5-day wound beds ($n \geq 6$ mice for each condition). (H) Composite ITGA6 immunostained images and quantification of re-epithelialization in 7-day wound beds. (I-J) Composite CD31 immunostained images (I) and quantification of the total CD31+ area in wound beds (I) and spatial distribution of CD31 (J) in wound beds 7 days after injury ($n = 5$ mice for each condition). White lines delineate wound edges. All scale bars, 250μm. Error bars indicate mean ± SEM.

Figure S3

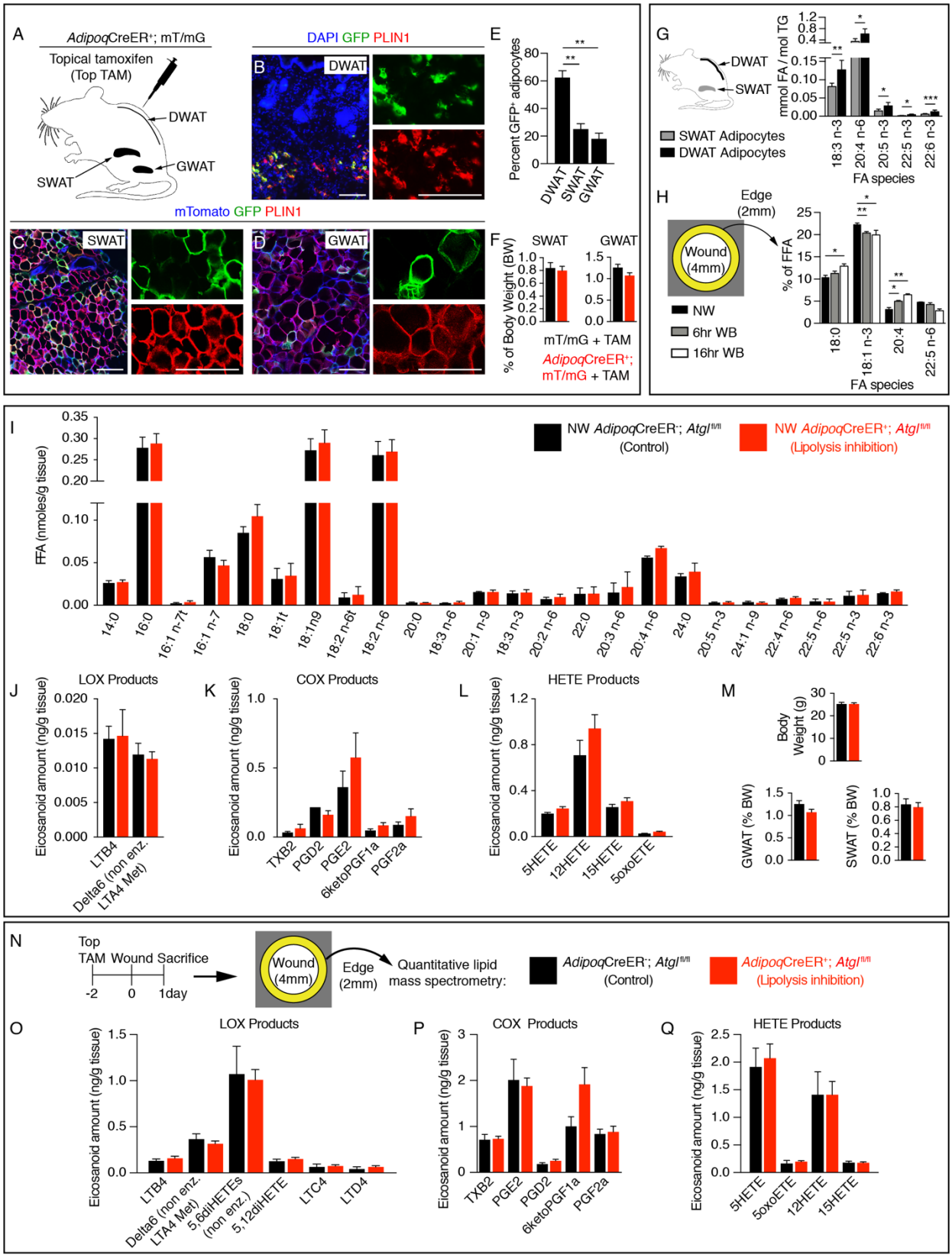
A
AdipoqCreER+; mT/mG
Topical tamoxifen (Top TAM)
DWAT
GWAT
SWAT
DAPI GFP PLIN1
B DWAT
mTomato GFP PLIN1
C SWAT
D GWAT
E
Percent GFP+ adipocytes
DWAT SWAT GWAT
F
SWAT GWAT
% of Body Weight (BW)
mT/mG + TAM
AdipoqCreER+; mT/mG + TAM
G
DWAT
SWAT
SWAT Adipocytes
DWAT Adipocytes
mmol FA / mol TG
18:3 n-3 20:4 n-6 20:5 n-3 22:5 n-3 22:6 n-3
FA species
H
Edge (2mm)
Wound (4mm)
NW
6hr WB
16hr WB
% of FFA
18:0 18:1 n-3 20:4 22:5 n-6
FA species
I
NW AdipoqCreER-; Atgl fl/fl (Control)
NW AdipoqCreER+; Atgl fl/fl (Lipolysis inhibition)
FFA (nmoles/g tissue)
14:0 16:0 16:1 n-7t 16:1 n-7 18:0 18:1t 18:1n9 18:2 n-6t 18:2 n-6 20:0 18:3 n-6 20:1 n-9 18:3 n-3 20:2 n-6 22:0 20:3 n-6 20:4 n-6 24:0 20:5 n-3 24:1 n-9 22:4 n-6 22:5 n-6 22:5 n-3 22:6 n-3
J
LOX Products
Eicosanoid amount (ng/g tissue)
LTB4
Delta6 (non enz.) LTA4 Met)
K
COX Products
TXB2 PGD2 PGE2 6ketoPGF1a PGF2a
L
HETE Products
5HETE 12HETE 15HETE 5oxoETE
M
Body Weight (g)
GWAT (% BW)
SWAT (% BW)
N
Top
TAM Wound Sacrifice
-2 0 1day
Wound (4mm)
Edge (2mm)
Quantitative lipid mass spectrometry:
AdipoqCreER-; Atgl fl/fl (Control)
AdipoqCreER+; Atgl fl/fl (Lipolysis inhibition)
O
LOX Products
LTB4
Delta6 (non enz.) LTA4 Met)
5,6diHETEs (non enz.)
5,12diHETE
LTC4
LTD4
P
COX Products
TXB2 PGE2 PGD2 6ketoPGF1a PGF2a
Q
HETE Products
5HETE 5oxoETE 12HETE 15HETE

Figure S3. Dermal adipocyte-derived lipids are not required for eicosanoid production during early inflammation. Related to Figure 2.

(A) Schematic of topical tamoxifen administration and location of adipose depots analyzed in *Adipoq*CreER; mT/mG mice. (B-D) GFP and PLIN1 immunostained sections from dermal (DWAT), subcutaneous (SWAT) and gonadal (GWAT) white adipose tissue. Scale bars, 100μm. (E) Quantification of the number of PLIN1+ cells that are GFP+ in *Adipoq*CreER; mT/mG mice receiving topical tamoxifen onto back skin (n = 4 mice). (F) Quantification of the percentage of total mouse weight that is SWAT and GWAT (n = 4-5 mice for each condition). (G) Quantitative lipid mass spectrometry of fatty acid species stored as triglycerides within adipocytes from dermal white adipose tissue (DWAT) and subcutaneous white adipose tissue (SWAT) (n = 6 mice for each depot). (H) Quantification of inflammatory free fatty acids at the wound edge following injury (n = 3 mice for each time point). (I-L) Quantitative lipid mass spectrometry of free fatty acids (I) and various eicosanoids (J-L) in uninjured skin from *Adipoq*CreER-; *Atgl*$^{fl/fl}$ and *Adipoq*CreER+; *Atgl*$^{fl/fl}$ mice (n = 4 mice for each condition). (M) Quantification of total body weight and the percentage of body weight that is GWAT and SWAT from uninjured *Adipoq*CreER-; *Atgl*$^{fl/fl}$ and *Adipoq*CreER+; *Atgl*$^{fl/fl}$ mice ($n \geq 5$ mice for each condition). (N-Q) Experimental paradigm (N) and quantitative lipid mass spectrometry various eicosanoids (O-Q) in the tissue surrounding wound beds 24 hours after injury (n = 4-5 mice for each time point). Error bars indicate mean ± SEM. *, $p < 0.05$; **, $p < 0.01$; ***, $p < 0.001$.

Figure S4

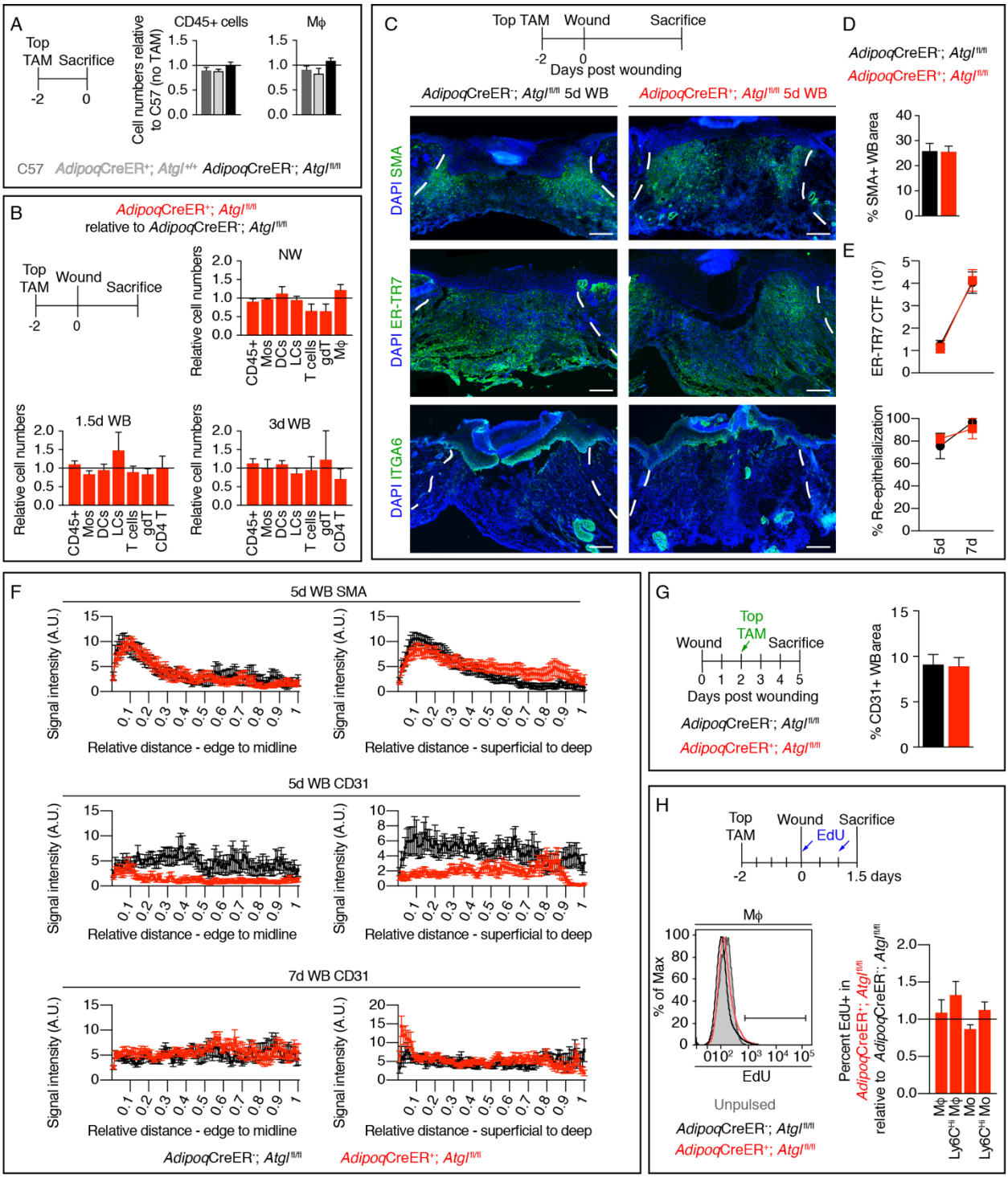
A
Top TAM
Sacrifice
-2
0
Cell numbers relative to C57 (no TAM)
CD45+ cells
Mϕ
C57 AdipoqCreER+; Atgl+/+ AdipoqCreER-; Atgl fl/fl
B
AdipoqCreER+; Atgl fl/fl relative to AdipoqCreER-; Atgl fl/fl
Top TAM
Wound
Sacrifice
NW
1.5d WB
3d WB
Relative cell numbers
CD45+
Mos
DCs
LCs
T cells
gdT
Mϕ
CD4 T
C
Top TAM
Wound
Sacrifice
Days post wounding
AdipoqCreER-; Atgl fl/fl 5d WB
AdipoqCreER+; Atgl fl/fl 5d WB
DAPI SMA
DAPI ER-TR7
DAPI ITGA6
D
AdipoqCreER-; Atgl fl/fl
AdipoqCreER+; Atgl fl/fl
% SMA+ WB area
E
ER-TR7 CTF (10⁷)
% Re-epithelialization
5d
7d
F
5d WB SMA
5d WB CD31
7d WB CD31
Signal intensity (A.U.)
Relative distance - edge to midline
Relative distance - superficial to deep
AdipoqCreER-; Atgl fl/fl
AdipoqCreER+; Atgl fl/fl
G
Top TAM
Wound
Sacrifice
Days post wounding
% CD31+ WB area
H
Top TAM
Wound
Sacrifice
EdU
-2
0
1.5 days
Mϕ
% of Max
EdU
Unpulsed
Percent EdU+ in AdipoqCreER+; Atgl fl/fl relative to AdipoqCreER-; Atgl fl/fl
Mϕ
Ly6C^hi Mϕ
Mo
Ly6C^hi Mo

Figure S4. Fibroblast repopulation and re-epithelialization are not delayed when dermal adipocyte lipolysis is inhibited. Related to Figure 3.

(A) Normalized quantification of immune cells and macrophages in uninjured skin treated with tamoxifen, relative to untreated C57 skin (*n* = 3-4 mice for each condition). (B) Normalized quantification of immune cell subsets in non-wounded skin (NW) (*n* = 6 mice for each condition), and wound beds 1.5 days (*n* = 6 mice for each condition) and 3 days (*n* = 4 mice for each condition) after injury. (C) Composite images from tissue sections immunostained for SMA, ER-TR7 and ITGA6 in day 5 wound beds. Scar bar, 250μm. White lines delineate wound edges. (D) Quantification of SMA in 5 day wound beds and (E) Quantification of ER-TR7 intensity and ITGA6 in 5- and 7-day wound beds of control (*Adipoq*CreER-; *Atgl*$^{fl/fl}$) and dermal adipocyte lipolysis inhibited (*Adipoq*CreER+; *Atgl*$^{fl/fl}$) mice (*n* = 6 mice for 5 day wounds; *n* = 3 mice for 7 day wounds). (F) Mean relative intensity of SMA in 5-day wound beds and CD31 in 5- and 7-day wound beds of *Adipoq*CreER-; *Atgl*$^{fl/fl}$ and *Adipoq*CreER+; *Atgl*$^{fl/fl}$ mice (*n* ≥ 6 mice for each condition and time point). (G) Quantification of CD31 immunostained tissue sections from day 5 wound beds or mice treated with tamoxifen 2 days after injury (*n* ≥ 5 mice for each condition). (H) Schematic of tamoxifen and EdU treatment. Flow cytometry plot and quantification of EdU-incorporating macrophages and monocytes in 1.5-day wound beds of *Adipoq*CreER-; *Atgl*$^{fl/fl}$ and *Adipoq*CreER+; *Atgl*$^{fl/fl}$ mice (*n* = 4 mice for each condition). Error bars indicate mean ± SEM. Mϕ, macrophage; Mo, monocyte; DC, dendritic cell; LC, Langerhans cell; gd T, gamma-delta T cell; NW, non-wounded; WB, wound bed.

Figure S5

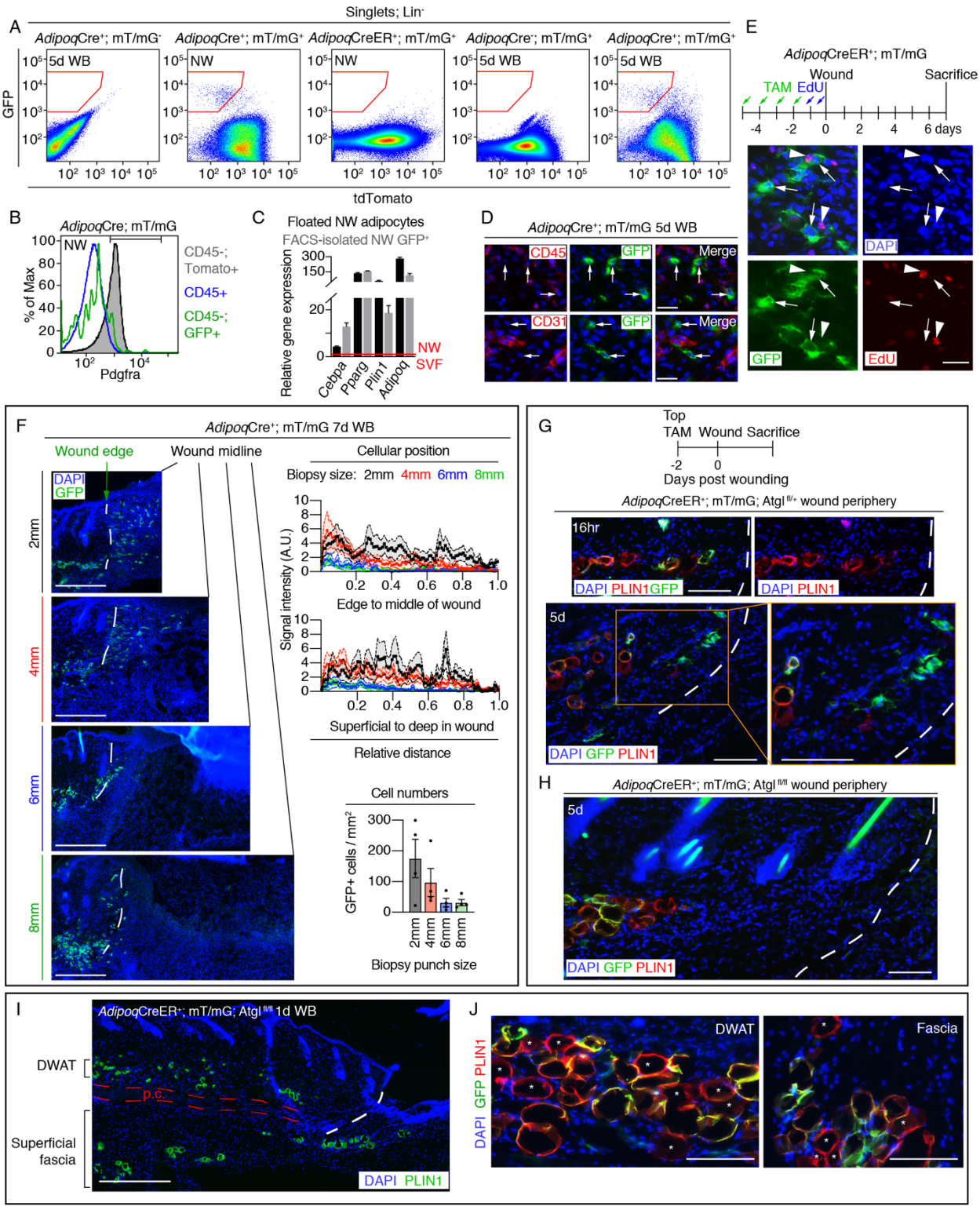
A
Singlets; Lin-
AdipoqCre+; mT/mG-
AdipoqCre+; mT/mG+
AdipoqCreER+; mT/mG+
AdipoqCre-; mT/mG+
AdipoqCre+; mT/mG+
5d WB
NW
GFP
tdTomato
B
AdipoqCre; mT/mG
% of Max
Pdgfra
CD45-; Tomato+
CD45+
CD45-; GFP+
C
Floated NW adipocytes
FACS-isolated NW GFP+
Relative gene expression
Cebpa
Pparg
Plin1
Adipoq
NW
SVF
D
AdipoqCre+; mT/mG 5d WB
CD45
CD31
GFP
Merge
E
AdipoqCreER+; mT/mG
Wound
Sacrifice
TAM EdU
-4 -2 0 2 4 6 days
DAPI
GFP
EdU
F
AdipoqCre+; mT/mG 7d WB
Wound edge
Wound midline
Cellular position
Biopsy size: 2mm 4mm 6mm 8mm
2mm
4mm
6mm
8mm
DAPI GFP
Signal intensity (A.U.)
Edge to middle of wound
Superficial to deep in wound
Relative distance
Cell numbers
GFP+ cells / mm2
Biopsy punch size
G
Top
TAM Wound Sacrifice
-2 0
Days post wounding
AdipoqCreER+; mT/mG; Atgl fl/+ wound periphery
16hr
5d
DAPI PLIN1 GFP
DAPI PLIN1
DAPI GFP PLIN1
H
AdipoqCreER+; mT/mG; Atgl fl/fl wound periphery
I
AdipoqCreER+; mT/mG; Atgl fl/fl 1d WB
DWAT
Superficial fascia
p.c.
DAPI PLIN1
J
DWAT
Fascia
DAPI GFP PLIN1

Figure S5. Wound edge dermal adipocyte-derived cells migrate into wound beds following lipid mobilization. Related to Figure 4 and Figure 5.

(A) Flow cytometry plots of GFP+ cells in back skin (NW) and wound beds from *Adipoq*Cre+; mT/mG and *Adipoq*CreER+; mT/mG mice given tamoxifen 7 days before analysis. (B) Flow cytometry plot of Pdgfra colocalization in cell populations from *Adipoq*Cre+; mT/mG mouse skin. (C) Quantitative real-time PCR of adipocyte-related genes in adipocytes and GFP+ cells isolated from *Adipoq*Cre+; mT/mG back skin. Red bar indicates gene expression of the dermal stromal vascular fraction (*n* = 3 mice). (D) Immunostained images of GFP and lineage markers (CD31 and CD45) in day 5 wound beds. White arrows indicate GFP+ cells. Scale bars, 25μm. (E) Labeling strategy and immunostained section showing GFP+ cells in the wound bed of *Adipoq*CreER+; mT/mG mice given EdU prior to wounding. Arrows indicate GFP+ cells and arrowheads indicate EdU+ cells. Scale bar, 25μm. (F) Composite images and quantification of the distribution and numbers of GFP+ cells in 7-day wounds of *Adipoq*Cre+; mT/mG mice. Original wounds were made with either a 2, 4, 6, or 8mm biopsy punch (*n* = 4 mice for each wound size). Scale bars, 500μm. (G-H) Images of GFP and PLIN1 immunostaining at the wound edge of 16-hour and 5-day wound beds from *Adipoq*CreER+; $Atgl^{fl/+}$ mice (G) and 5-day *Adipoq*CreER+; $Atgl^{fl/fl}$ mice (H). Scale bars, 100μm. (I-J) Low magnification image of PLIN1 immunostained tissue at the wound edge (I) and higher magnification images of GFP and PLIN1 colocalization in the DWAT and adipocytes located in the deeper fascia (J). Red dotted line delineates the panniculus carnosus (p.c.). Asterisks indicates GFP-; PLIN1+ cells. Scale bars, 500μm (I) and 100μm (J). White dotted lines delineate wound edges. Error bars indicate mean ± SEM. SVF, stromal vascular fraction; WB, wound bed.

Figure S6

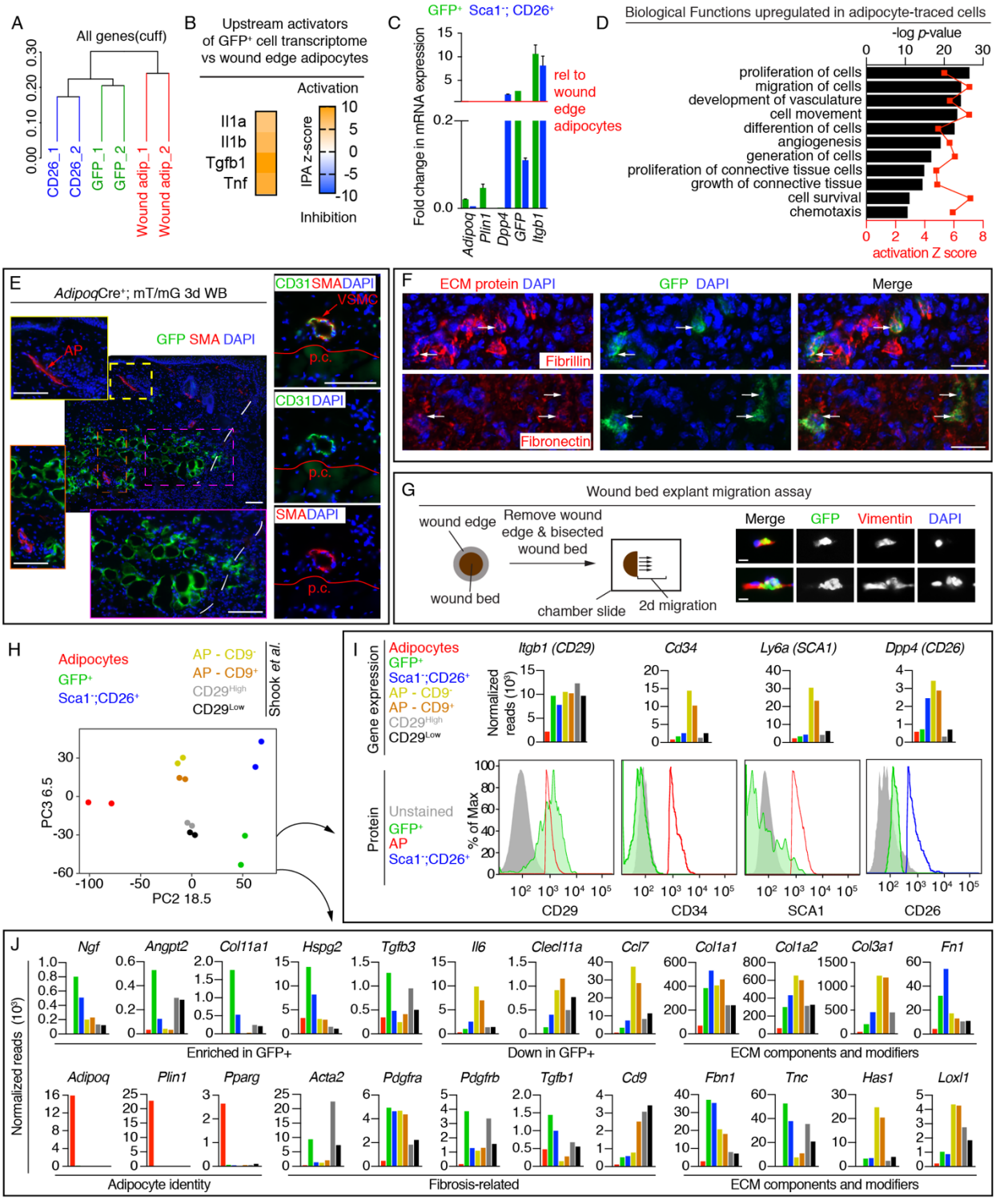
A
All genes(cuff)
0.00 0.10 0.20 0.30
CD26_1
CD26_2
GFP_1
GFP_2
Wound adip_1
Wound adip_2
B
Upstream activators of GFP+ cell transcriptome vs wound edge adipocytes
Activation
Il1a
Il1b
Tgfb1
Tnf
IPA z-score
10 5 0 -5 -10
Inhibition
C
GFP+ Sca1-; CD26+
Fold change in mRNA expression
15 10 5
0.2
0.0
rel to wound edge adipocytes
Adipoq Plin1 Dpp4 GFP Itgb1
D
Biological Functions upregulated in adipocyte-traced cells
-log p-value
0 10 20 30
proliferation of cells
migration of cells
development of vasculature
cell movement
differention of cells
angiogenesis
generation of cells
proliferation of connective tissue cells
growth of connective tissue
cell survival
chemotaxis
0 2 4 6 8
activation Z score
E
AdipoqCre+; mT/mG 3d WB
AP
GFP SMA DAPI
CD31SMADAPI
VSMC
p.c.
CD31DAPI
SMADAPI
F
ECM protein DAPI
GFP DAPI
Merge
Fibrillin
Fibronectin
G
Wound bed explant migration assay
wound edge
wound bed
Remove wound edge & bisected wound bed
chamber slide
2d migration
Merge GFP Vimentin DAPI
H
Adipocytes
GFP+
Sca1-;CD26+
AP - CD9-
AP - CD9+
CD29High
CD29Low
Shook et al.
PC3 6.5
PC2 18.5
I
Gene expression
Adipocytes
GFP+
Sca1-;CD26+
AP - CD9-
AP - CD9+
CD29High
CD29Low
Normalized reads (10³)
Itgb1 (CD29)
Cd34
Ly6a (SCA1)
Dpp4 (CD26)
Protein
Unstained
GFP+
AP
Sca1-;CD26+
% of Max
CD29
CD34
SCA1
CD26
J
Normalized reads (10³)
Ngf
Angpt2
Col11a1
Hspg2
Tgfb3
Il6
Clecl11a
Ccl7
Col1a1
Col1a2
Col3a1
Fn1
Enriched in GFP+
Down in GFP+
ECM components and modifiers
Adipoq
Plin1
Pparg
Acta2
Pdgfra
Pdgfrb
Tgfb1
Cd9
Fbn1
Tnc
Has1
Loxl1
Adipocyte identity
Fibrosis-related
ECM components and modifiers

Figure S6. Adipocyte-derived cells have a unique myofibroblast gene expression profile. Related to Figure 6.

(A) Hierarchical clustering of cell populations from RNA-sequencing. (B) Ingenuity Pathway Analysis of the predicted upstream activators for the genes enriched in GFP+ cells relative to adipocytes. (C) Quantitative RT-PCR in cell populations isolated for RNA-seq experiments (*n* = 3 mice). (D) Predicted biofunctions upregulated by the gene expression profile of adiponectin-traced cells relative to mature adipocytes at the wound periphery. (E) SMA immunostained sections at the periphery of day 3 wound beds co-stained with GFP or CD31 in *Adipoq*Cre+; mT/mG mice. Colored dashed boxes show the area of higher magnification. Scale bars, 100μm. Red line indicates panniculus carnosus (p.c.). (F) Images from GFP immunostained sections from the center of 5-day wound beds from *Adipoq*Cre+; mT/mG mice co-stained with fibrillin or fibronectin. Arrow indicate GFP+ cells that colocalize with ECM proteins. Scale bars, 100μm. (G) Schematic and images of GFP+; Vimentin+ cells that migrated out day 5 wound beds from *Adipoq*Cre+; mT/mG mice (72/78 GFP+ cells were vimentin+, *n* = 4 wounds). Scale bars, 10μm. (H) Principal component (PC) analysis of wound-associated populations from Figure 6 with previously reported myofibroblast subsets. (I) Normalized read counts from RNA-seq experiments (top) and flow cytometry plots (bottom) of CD34, CD29, SCA1 and CD26 of GFP+ cells in 5-day wound beds. (J) Normalized read counts comparing gene expression of GFP+ cells to wound edge adipocytes and different subsets of day 5 wound bed myofibroblasts. Error bars indicate mean ± SEM. AP, arrector pili; VSMC, vascular smooth muscle cell.

Figure S7

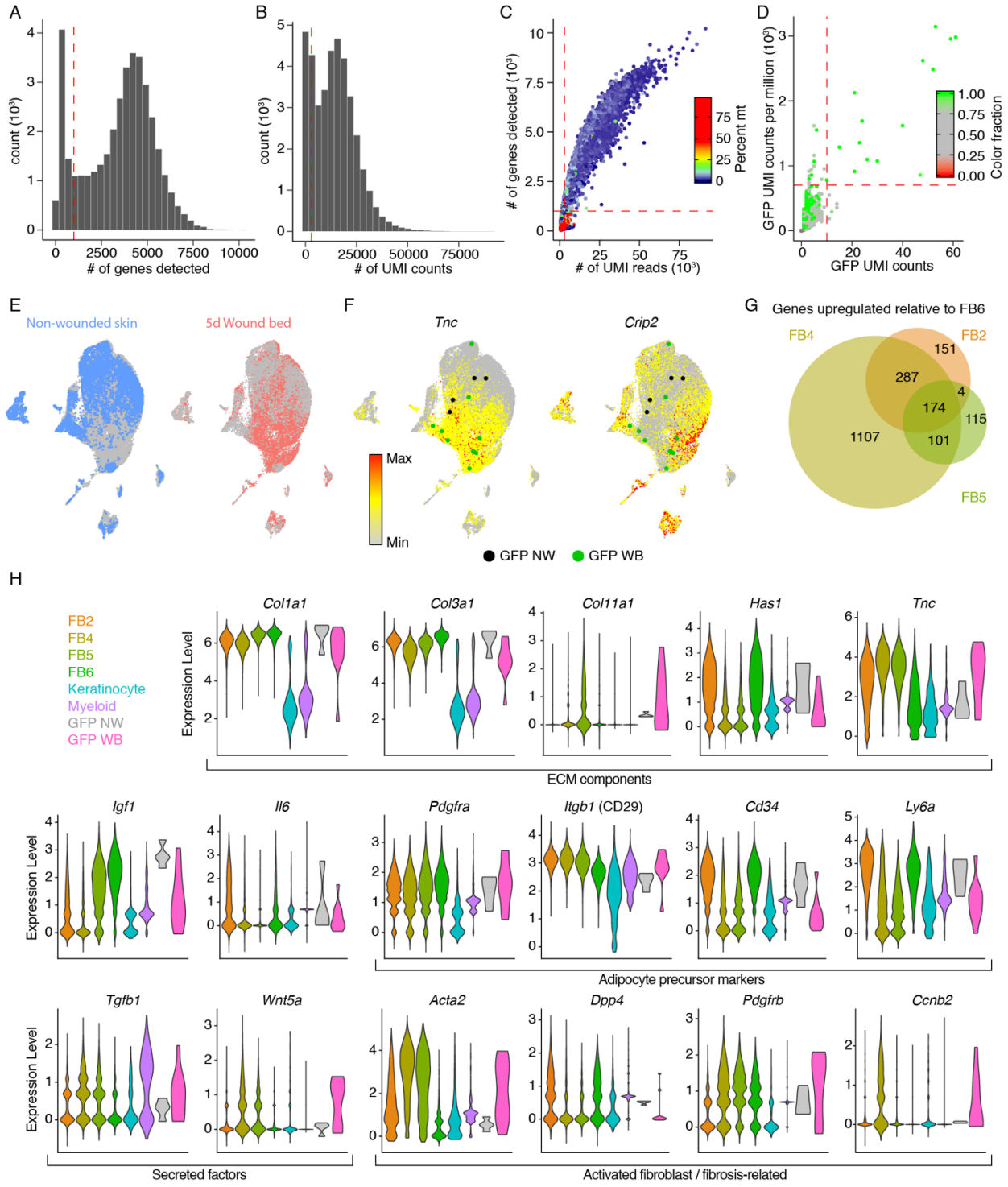
A
count (10³)
# of genes detected
B
count (10³)
# of UMI counts
C
# of genes detected (10³)
# of UMI reads (10³)
Percent mt
D
GFP UMI counts per million (10³)
GFP UMI counts
Color fraction
E
Non-wounded skin
5d Wound bed
F
Tnc
Crip2
Max
Min
GFP NW
GFP WB
G
Genes upregulated relative to FB6
FB4
FB2
FB5
151
287
4
174
115
1107
101
H
FB2
FB4
FB5
FB6
Keratinocyte
Myeloid
GFP NW
GFP WB
Expression Level
Col1a1
Col3a1
Col11a1
Has1
Tnc
ECM components
Igf1
Il6
Pdgfra
Itgb1 (CD29)
Cd34
Ly6a
Adipocyte precursor markers
Tgfb1
Wnt5a
Acta2
Dpp4
Pdgfrb
Ccnb2
Secreted factors
Activated fibroblast / fibrosis-related

Figure S7. Single cell RNA-seq analysis of wound bed myofibroblasts and *Adipoq*-traced cells. Related to Figure 7, Table S1 and Table S2.

(A,B) Histogram of the number of genes detected per barcode (A) and number of UMI counts per barcode (B) with cutoffs for inclusion for future analysis shown as a red vertical lines. Barcodes with fewer than 100 genes detected were excluded from this analysis. (C) Scatterplot of UMI reads versus number of genes detected per barcode, with the percentage of reads mapping to mitochondrial genes indicated on a color scale. Cutoffs for cell inclusion are indicated as dashed lines. (D) Scatterplot of the number of UMI counts mapping to GFP and the fraction of all UMIs mapping to GFP (expressed in counts per million). Cells are colored by the fraction of reads that map either to eGFP (green) or tdTomato (red). Cutoffs to identify confidently GFP+ cells are indicated as dashed lines. (E) UMAP plots showing the location of cells from non-wounded skin and wound beds. (F) Gene expression plots showing distribution of *Tnc and Crip2*. Expression levels for each cell are shown as Pearson residuals and displayed using a color scale, overlaid onto the UMAP plot. GFP+ cells from NW and WB samples are overlaid to emphasize their location. (G) Venn diagrams displaying the number of differentially expressed genes in selected fibroblast clusters relative to FB6, using the Wilcoxon rank sum test implemented through Seurat. (H) Violin plots of genes that functionally discriminate subsets of wound-associated fibroblast populations.